Supplemental Information for

# A Sulfonate Functionalized Viologen Enabling Neutral Cation Exchange Aqueous Organic Redox Flow Batteries towards Renewable Energy Storage

Camden DeBruler, Bo Hu, Jared Moss, Jian Luo, and T. Leo Liu*

The Department of Chemistry and Biochemistry, Utah State University, Logan, UT

*Corresponding Author: Leo.Liu@usu.edu

## Experimental

**Chemicals and instrumentation:** All chemicals were purchased from TCI or Sigma-Aldrich and used as received. All experiments were performed under an $N_2$ atmosphere. NMR spectra were collected on a Bruker 500 MHz spectrometer at 25 ˚C. Elemental analysis was performed by Atlantic Microlab. All electrochemical experiments were conducted with a Gamry 5000e potentiostat. Conductivity of the electrolyte solutions was measured using a Mettler Toledo conductivity meter at R.T. Battery testing was performed using a Lanhe battery testing system.

**Synthesis of 1,1'-bis[3-sulfonatoethyl]-4,4'-bipyridinium ($(SEt)_2V$).** In a 100 mL $N_2$ purged Schlenk flask, 4,4'-bipyridine (2.0 g, 12.8 mmol) and 3-sulfonatoethyl bromide (5.4 g, 25.6 mmol) was dissolved in 50 mL DMSO, and the reaction mixture was stirred at 140 °C. After 48 h, the reaction solution was cooled to room temperature, and concentrated to 10 mL. 50 mL $CH_3CN$ was added to generate white precipitate. The white precipitate was washed with 20 mL $CH_3CN$ and dried under vacuum to give a yield of 15%. 1H NMR studies of the combined $CH_3CN$ solution confirmed ca. 73% unreacted 4,4'-bipyridine. $^1$H NMR (500 MHz, $d_6$-DMSO), δ 9.21 (d, $J$ = 2.5 Hz, 4H), 8.61 (d, $J$ = 2.5 Hz, 4H), 3.65 (t, $J$ = 5.2 Hz, 4H), 3.01 (t, $J$ = 5.2 Hz, 4H).

**Synthesis of 1,1'-bis[3-sulfonatopropyl]-4,4'-bipyridinium ($(SPr)_2V$).** Although $(SPr)_2V$ was synthesized before,[1,2] the reported reaction conditions and yields need further improvement. In a 250 mL $N_2$ purged Schlenk flask, propane sultone (4.7 g, 38.4 mmol) was dissolved in 35 mL toluene and brought to reflux. 4,4'-bipyridine (3.0 g, 19.2 mmol) was dissolved in 25 mL toluene, and added dropwise to the refluxing solution. After 3 h at 110 °C, the flask was cooled to room temperature. The resulting white precipitate was filtered, washed with 30 mL acetonitrile, and dried under vacuum. 6.8 g, 98% yield. When the reaction was scaled up to a 20 g scale, the isolation yield was 100%. $^1$H NMR (500 MHz, $D_2O$) δ 9.04 (d, $J$ = 5.8 Hz, 4H), 8.45 (d, $J$ = 5.7 Hz, 4H), 4.78 (t, $J$ = 7.2 Hz, 4H), 2.91 (t, $J$ = 7.0 Hz, 4H), 2.46 – 2.37 (m, 4H). Elemental analysis for $C_{16}H_{20}N_2O_6S_2$, Calculated: C 47.99, H 5.03, N 7.00. Found: C 47.97, H 5.06, N 6.86.

**Cyclic Voltammetry Studies:** All CV tests were performed with a Gamry 5000e potentiostat using a three-electrode system in a 0.5 M KCl electrolyte solution under $N_2$ atmosphere. The working electrode consisted of a PEEK-encased 1 mm diameter glassy carbon disk. A glassy carbon rod served as the counter electrode. An Ag/AgCl reference electrode was constructed by submerging a silver wire in 3.0 M KCl solution. Before each experiment, the working electrode was polished with 0.05-micron alumina powder and rinsed with deionized water. Potential values were corrected to NHE using a (ferrocenylmethyl)trimethylammonium chloride internal standard with a known redox potential at 0.61 V vs. NHE.

**Electrochemical RDE studies:** Linear sweep voltammetry (LSV) experiments were conducted using a Gamry 5000e potentiostat with a three-electrode system. The working electrode consisted of a rotating 5 mm glassy carbon disk encased in teflon. The working electrode was cleaned using the same method as in the CV experiments. The counter and reference electrodes are the same as in the CV experiments. During each scan, the working electrode rotated from 300

rpm to 2400 rpm at increments of 300 rpm. Three scans at each rotation rate were collected to ensure accuracy. **$(SPr)_2V$**: LSV scans were collected in 0.5 M KCl supporting electrolyte at a rate of 5 mV/s from -0.3 V to -0.6 V versus NHE. The limiting currents (mass transport-limited current intensity) at each rotation rate were recorded at -0.6 V versus NHE. The Levich plot of limiting current versus square root rotation rate showed a linear relationship. The slope of the fitted line is defined by the Levich equation,

$$\text{Levich Plot Slope} = 0.620nFAC_0D^{2/3}\nu^{-1/6} \qquad \text{(Equation S1)}$$

where n = 1 for a single electron process, Faraday's constant F = 96485 C/mol, electrode area A = 0.1963 $cm^2$, **$(SPr)_2V$** concentration $C_0$ = 1 x $10^{-6}$ mol/$cm^3$, D represents the diffusion coefficient, and the kinematic viscosity of 0.5 M KCl aqueous solution $\nu$ = 0.0088 $cm^2$/s. The diffusion coefficient of **$(SPr)_2V$** was determined as 3.26 x $10^{-6}$ $cm^2$/s.

**Nicholson's method to estimate electron transfer rates constant:** Following the well-known Nicholson's method,[3] the peak($E_{pc}$)-peak($E_{pa}$) separation, $\Delta E_p$, was used to obtain the kinetic parameter, $\Psi$, and then equation S2 was applied to calculate $k^0$. The reduction of **$(SPr)_2V$** displayed a nearly constant $\Delta E_p$ around 57 mV from 5 to 500 mV/s (Figure S2), confirming a fast and reversible Nernst reduction process. For Nicholson's method, $\Delta E_p$ has a limit value of 61 mV, corresponding to $\Psi$ as 20. Thus, a higher low-bound limit of $k^0$ for the reduction of **$(SPr)_2V$** was estimated using $\Psi$ = 20, scan rate at 500 mV/s, and corresponding diffusion constants. $k^0$ of the reduction is therefore greater than 0.28 cm/s.

$$k^0 = \Psi[\pi Dn\nu F/RT]^{1/2} \qquad \text{(Equation S2)}$$

where F, D, and n are defined in Equation S1, and $\nu$ represents the scan rate.

**Flow Cell Tests:** The flow cells were constructed from two machined graphite chambers. In each chamber was a graphite felt electrode (SGL Carbon Group, Germany). A sheet of cation

exchange membrane was sandwiched between the graphite chambers with an active area of 10 $cm^2$. On the exterior of each half-cell was a copper current collector. Electrolyte flow was facilitated by a Masterflex® L/S® peristaltic pump operating at 60 mL/min. The $(SPr)_2V$ / KI AORFBs: each reservoir contained 12 ml of electrolyte solution. The anode consisted of 0.5 M **$(SPr)_2V$** and 2.0 M KCl. The cathode consisted of 2.0 M KI and 2.0 M KCl. The battery was galvanostatically cycled between 1.25 V and 0.30 V at current densities of 40, 60, 80, and 100 $mA/cm^2$. Nation 212 or Selemin CSO membrane was applied in the battery studies. According the vendor of the Selemin CSO membrane, the bulk price of the CSO membrane is ca. $100/$m^2$. The extended cycling test was performed at 60 $mA/cm^2$ for 300 cycles for Nafion 212 membrane and 100 cycles for the CSO membrane. After cycling, the battery was fully discharged, and samples of the anode and cathode were collected and tested to measure the chemical stability and crossover of the active materials by CV and $^1$H NMR.

**Computational Methods:** Calculations for the ground-state structures and mapping the electrostatic potentials of **$(SPr)_2V^0$** and **$(SPr)_2V^-$** were performed using the Gaussian 09 package.[4] Both compounds were modeled as isolated molecules at 298 K. The two oxidation states were optimized using the 6-31+G(d) basis sets[5,6] and the M06-2x electron correlation method (Minnesota '06 2x global hybrid functional with 54% HF exchange).[7] The aqueous solvent was modeled using the SMD[8] universal solvation model which is based on the quantum mechanical charge density of a solute molecule interacting with a continuum description of the solvent. Energy minimum of each optimized structure was confirmed by frequency calculation using the Chemcraft software. This software was also used to view the electrostatic potential mapping of each molecule.

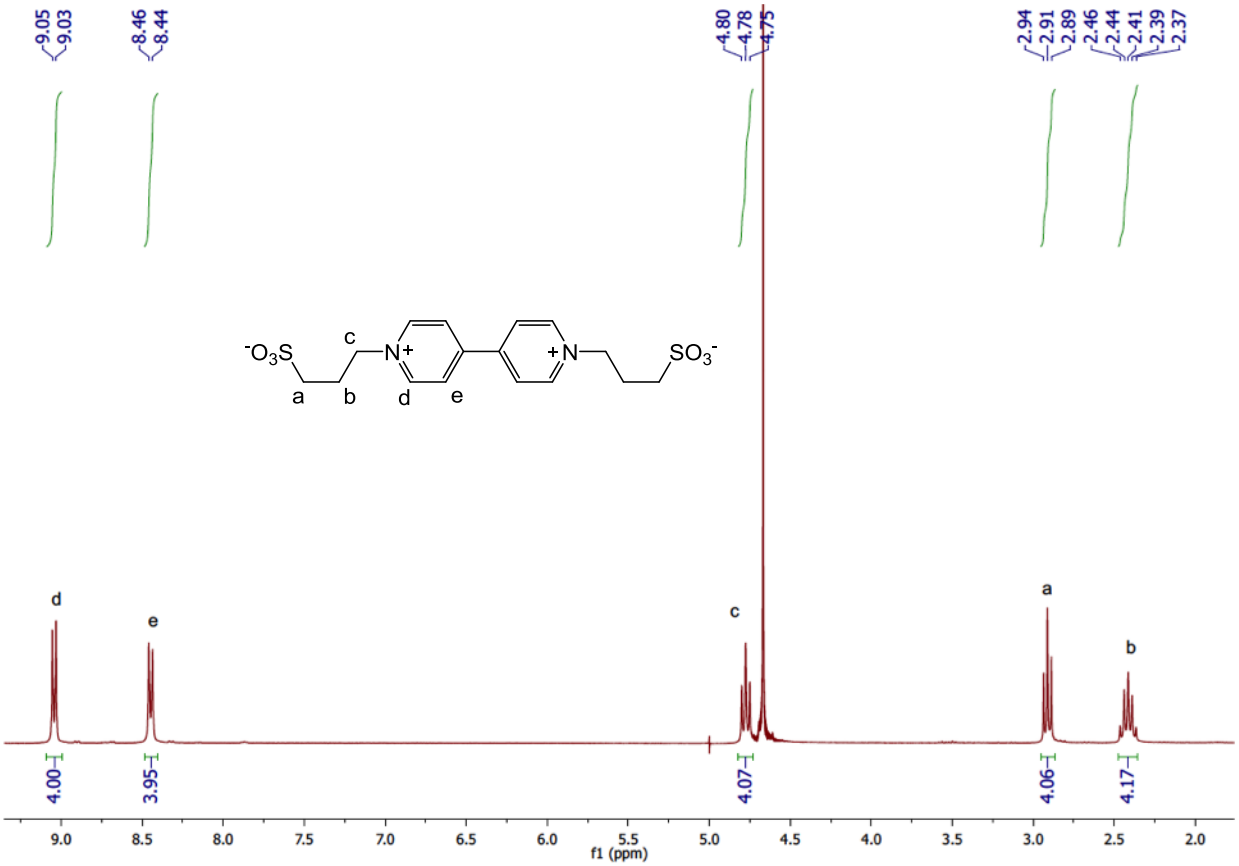


**Figure S1**. $^{1}$H NMR spectrum of **(SPr)$_2$V**. Conditions: 500 MHz field strength, 25 °C, $D_2O$ solvent. The residual HOD solvent peak is observed ~4.75 ppm. The structure has been labeled, assigning each individual peak in the spectrum.

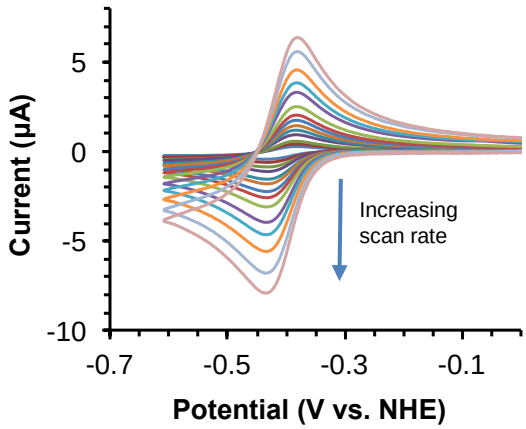


**Figure S2**: CV curves of **$(SPr)_2V$** at varied scan rates for Nicholson analysis. Conditions: 2 mL of 1 mM **$(Spr)_2V$** in 0.5 M KCl supporting electrolyte. CV collected at scan rates of 5, 10, 20, 40, 70, 100, 150, 200, 300, and 500 mV/s. Glassy carbon working and counter electrodes. Ag/AgCl reference electrode. The working electrode was polished between each scan to ensure accuracy.

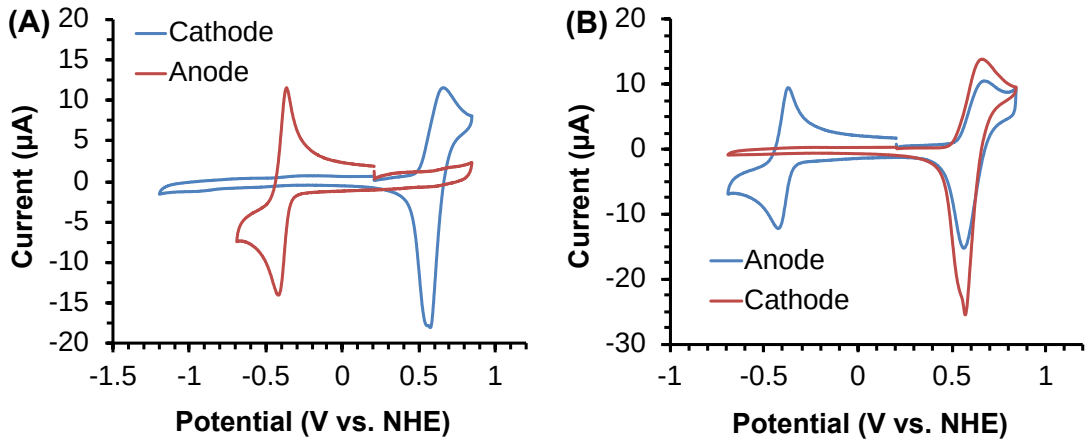


**Figure S3.** Post-cycling CV analysis of anode and cathode solutions from RFB's employing Nafion 212 membrane (A), and Selemion CSO membrane (B). Conditions: active material in each anode or cathode electrolyte diluted to 4 mM in 0.5 M NaCl supporting electrolyte, 100 mV/s scan rate, glassy carbon working electrode, glassy carbon counter electrode, silver/silver chloride reference electrode.

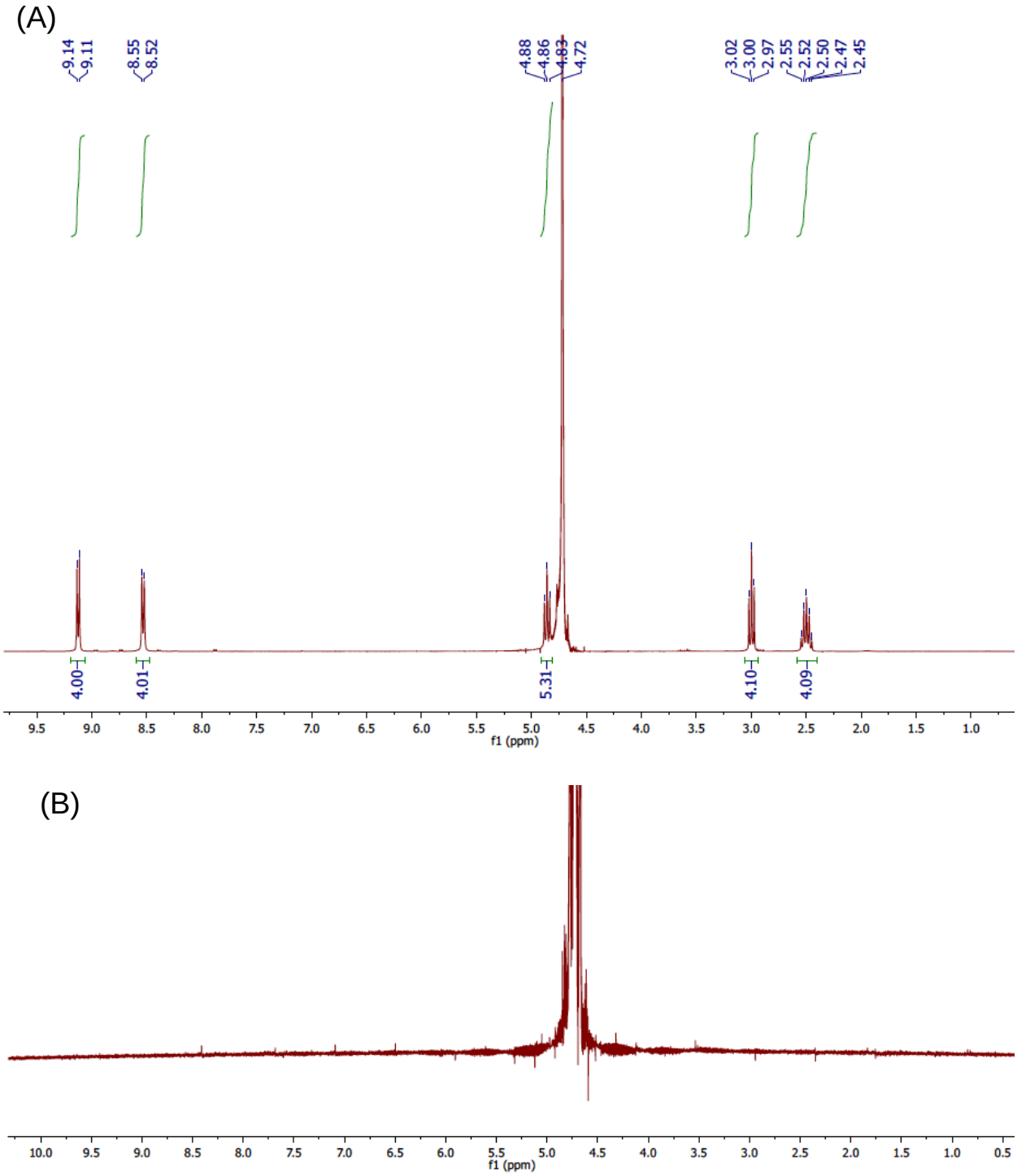


**Figure S4.** Post-cycling $^{1}$H NMR analysis of anode electrolyte (A) and cathode electrolyte (B) using Nafion 212 membrane. Conditions: 20 µL electrolyte diluted into 600 µL $D_2O$. Residual $H_2O$ from the electrolyte causes a strong solvent absorption at 4.72 ppm. The signal intensity in (B) was increased to show no detectable **$(SPr)_2V$** within the noise threshold of the instrument.

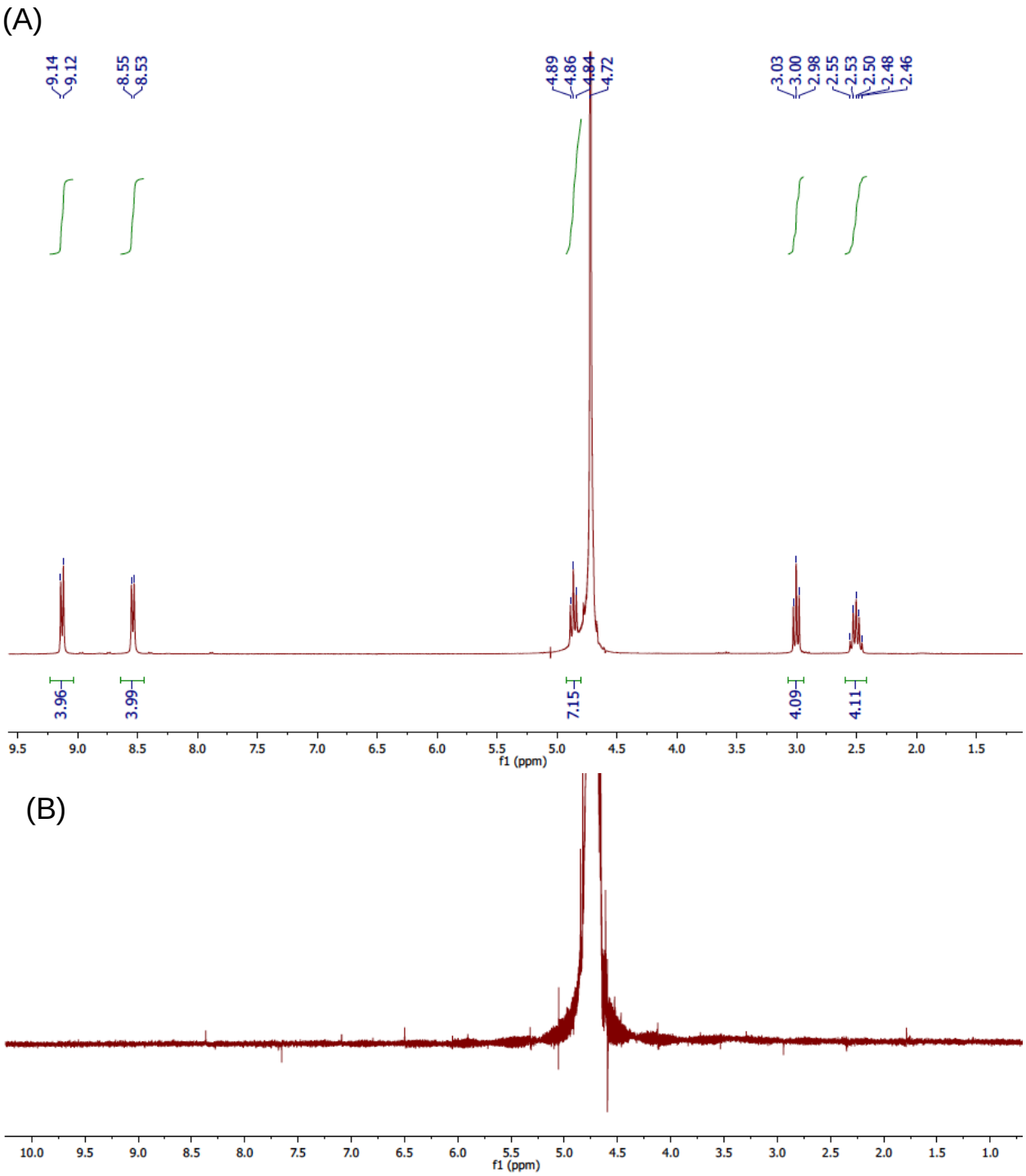


**Figure S5.** Post-cycling $^{1}H$ NMR analysis of anode electrolyte (A) and cathode electrolyte (B) using Selemion CSO membrane. Conditions: 20 μL electrolyte diluted into 600 μL $D_2O$. Residual $H_2O$ from the electrolyte causes a strong solvent absorption at 4.72 ppm. The signal

intensity in (B) was increased to show no detectable **(SPr)$_2$V** within the noise threshold of the instrument.

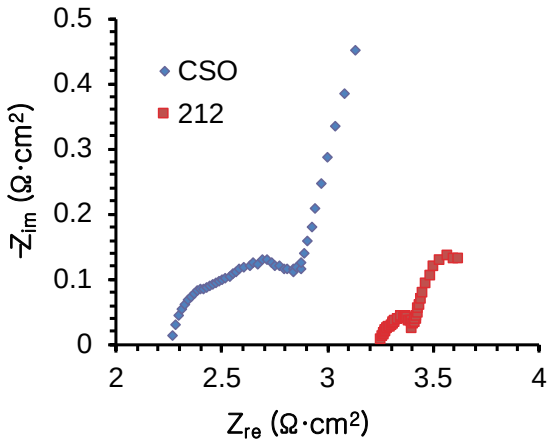


**Figure S6.** Nyquist plots of **(SPr$_2$)V** / KI RFB's using Nafion 212 or Selemion CSO membrane.

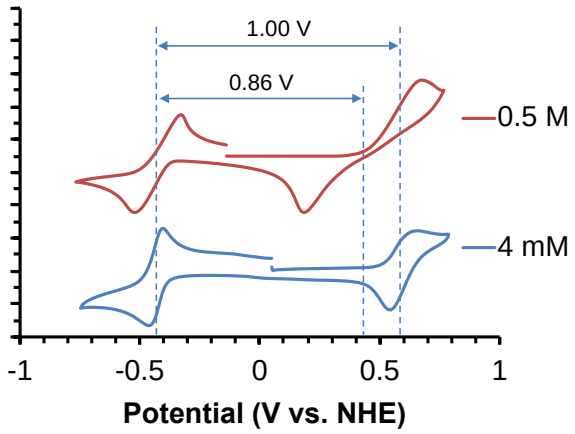


**Figure S7.** Cyclic voltammograms of 4 mM **(SPr$_2$)V** with 4 mM KI (blue trace), and 0.5 M **(SPr$_2$)V** with 0.5 M KI (red trace). At higher concentration, the iodide redox couple becomes less reversible, and $E_{1/2}$ shifts from +0.57 V to +0.43 V vs. NHE.

**Figure S8.** DFT optimized structure and coordinates of **(SPr$_2$)V**

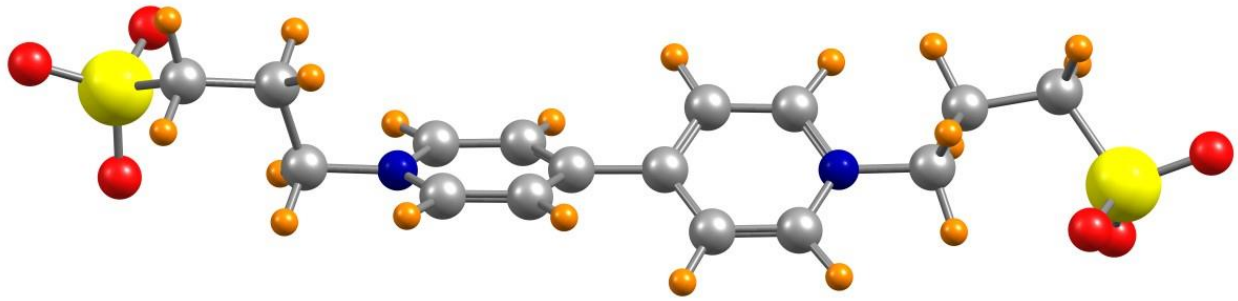

**(SPr)$_2$V Optimized Coordinates**

| | | | |
|---|---|---|---|
| 6 | 2.668888000 | 1.47306000 | -0.103738000 |
| 7 | 3.469269000 | 0.449324000 | -0.457978000 |
| 6 | 2.956257000 | -0.748201000 | -0.796892000 |
| 6 | 1.590468000 | -0.953425000 | -0.802039000 |
| 6 | 0.735571000 | 0.094776000 | -0.450078000 |
| 6 | 1.297005000 | 1.325935000 | -0.096870000 |
| 6 | -0.735534000 | -0.093675000 | -0.450261000 |
| 6 | -1.297015000 | -1.325111000 | -0.098096000 |
| 6 | -2.668893000 | -1.472738000 | -0.105116000 |
| 7 | -3.469245000 | -0.448144000 | -0.458541000 |
| 6 | -2.956187000 | 0.749622000 | -0.796543000 |
| 6 | -1.590388000 | 0.954817000 | -0.801452000 |
| 6 | 4.941342000 | 0.628091000 | -0.403337000 |
| 6 | 5.434466000 | 0.388283000 | 1.020233000 |
| 6 | 6.903944000 | 0.737898000 | 1.219373000 |
| 16 | 8.036231000 | -0.232593000 | 0.216977000 |
| 6 | -4.941309000 | -0.626974000 | -0.403921000 |
| 6 | -5.434283000 | -0.388779000 | 1.019979000 |
| 6 | -6.903607000 | -0.739060000 | 1.218976000 |
| 16 | -8.036322000 | 0.231543000 | 0.217202000 |

| | | | |
|---|---|---|---|
| 8 | 7.618645000 | -1.653742000 | 0.368421000 |
| 8 | 7.891783000 | 0.250867000 | -1.185203000 |
| 8 | -7.891845000 | -0.251186000 | -1.185217000 |
| 8 | -9.391296000 | -0.036009000 | 0.770500000 |
| 1 | -7.110902000 | -1.787567000 | 0.983219000 |
| 1 | -7.191102000 | -0.551842000 | 2.257003000 |
| 1 | -5.252652000 | 0.653703000 | 1.301720000 |
| 1 | -4.857723000 | -1.022204000 | 1.703881000 |
| 1 | -5.369993000 | 0.077175000 | -1.116610000 |
| 1 | -5.153319000 | -1.644710000 | -0.739030000 |
| 1 | 5.369908000 | -0.075217000 | -1.116917000 |
| 1 | 5.153340000 | 1.646219000 | -0.737263000 |
| 1 | 4.858169000 | 1.021241000 | 1.704802000 |
| 1 | 7.111602000 | 1.786464000 | 0.984202000 |
| 1 | 7.191426000 | 0.549936000 | 2.257267000 |
| 1 | 5.252538000 | -0.654410000 | 1.300990000 |
| 1 | 3.162760000 | 2.400631000 | 0.166623000 |
| 1 | 0.685131000 | 2.169851000 | 0.200886000 |
| 1 | 1.212853000 | -1.924478000 | -1.102429000 |
| 1 | 3.667414000 | -1.521353000 | -1.064174000 |
| 1 | -1.212713000 | 1.926099000 | -1.101051000 |
| 1 | -3.667309000 | 1.523001000 | -1.063261000 |
| 1 | -3.162790000 | -2.399972000 | 0.164481000 |
| 1 | -0.685183000 | -2.169292000 | 0.198992000 |
| 8 | 9.391368000 | 0.034172000 | 0.770238000 |
| 8 | -7.619219000 | 1.652757000 | 0.369276000 |

**Figure S9**. DFT optimized structure and coordinates of **$(SPr_2)V^-$**

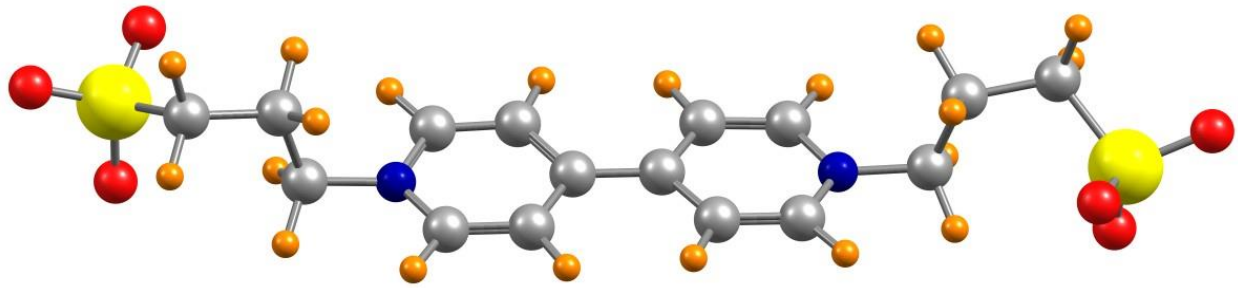

**$[(SPr)_2V]^-$ Optimized Coordinates**

| | | | |
|---|---|---|---|
| 6 | -2.710704000 | -1.459738000 | -0.561397000 |
| 7 | -3.517904000 | -0.358728000 | -0.569927000 |
| 6 | -2.951312000 | 0.881007000 | -0.492800000 |
| 6 | -1.597523000 | 1.049642000 | -0.458221000 |
| 6 | -0.709286000 | -0.072288000 | -0.485273000 |
| 6 | -1.350980000 | -1.351136000 | -0.526542000 |
| 6 | 0.709332000 | 0.072758000 | -0.485301000 |
| 6 | 1.351010000 | 1.351628000 | -0.526089000 |
| 6 | 2.710733000 | 1.460254000 | -0.560978000 |
| 7 | 3.517945000 | 0.359251000 | -0.569972000 |
| 6 | 2.951366000 | -0.880516000 | -0.493328000 |
| 6 | 1.597582000 | -1.049174000 | -0.458776000 |
| 6 | -4.978068000 | -0.506641000 | -0.512062000 |
| 6 | -5.452181000 | -0.566180000 | 0.938006000 |
| 6 | -6.925499000 | -0.921218000 | 1.095041000 |
| 16 | -8.057915000 | 0.236628000 | 0.318025000 |
| 6 | 4.978118000 | 0.507151000 | -0.512072000 |
| 6 | 5.452255000 | 0.566241000 | 0.938008000 |
| 6 | 6.925653000 | 0.920897000 | 1.095097000 |
| 16 | 8.057835000 | -0.237152000 | 0.318041000 |
| 8 | -7.614430000 | 1.599341000 | 0.723671000 |

| | | | |
|---|---|---|---|
| 8 | -7.958215000 | 0.023467000 | -1.152922000 |
| 8 | 7.958201000 | -0.023965000 | -1.152905000 |
| 8 | 9.406489000 | 0.108173000 | 0.845437000 |
| 1 | 7.156862000 | 1.900587000 | 0.664733000 |
| 1 | 7.199069000 | 0.932341000 | 2.153654000 |
| 1 | 5.239310000 | -0.388939000 | 1.430786000 |
| 1 | 4.879477000 | 1.340659000 | 1.461812000 |
| 1 | 5.411368000 | -0.340537000 | -1.045939000 |
| 1 | 5.240664000 | 1.421482000 | -1.050982000 |
| 1 | -5.411323000 | 0.341215000 | -1.045652000 |
| 1 | -5.240617000 | -1.420808000 | -1.051254000 |
| 1 | -4.879223000 | -1.340585000 | 1.461633000 |
| 1 | -7.156483000 | -1.900938000 | 0.664628000 |
| 1 | -7.198916000 | -0.932787000 | 2.153596000 |
| 1 | -5.239460000 | 0.388936000 | 1.431001000 |
| 1 | -3.218000000 | -2.417707000 | -0.600425000 |
| 1 | -0.781506000 | -2.272015000 | -0.544167000 |
| 1 | -1.229035000 | 2.066814000 | -0.405896000 |
| 1 | -3.642984000 | 1.716543000 | -0.471518000 |
| 1 | 1.229109000 | -2.066372000 | -0.406907000 |
| 1 | 3.643051000 | -1.716051000 | -0.472432000 |
| 1 | 3.218012000 | 2.418244000 | -0.599677000 |
| 1 | 0.781517000 | 2.272505000 | -0.543311000 |
| 8 | -9.406514000 | -0.108970000 | 0.845398000 |
| 8 | 7.614110000 | -1.599793000 | 0.723658000 |

**References**:


(1) Nagamura, T.; Kurihara, T.; Matsuo, T.; Sumitani, M.; Yoshihara, K. Novel effect of man-made molecular assemblies on photoinduced charge separation. 3. Sensitized photoreduction of zwitterionic viologen in the presence of cationic surfactants *J. Phys. Chem.* **1982**, *86*, 4368-4371.

(2) Bhandari, S.; Deepa, M.; Pahal, S.; Joshi, A. G.; Srivastava, A. K.; Kant, R. A Dual Electrochrome of Poly-(3,4-Ethylenedioxythiophene) Doped by N,N′ -Bis(3-sulfonatopropyl)-4-4′ -bipyridinium−Redox Chemistry and Electrochromism in Flexible Devices *ChemSusChem* **2010**, *3*, 97-105.

(3) Nicholson, R. S. Theory and Application of Cyclic Voltammetry for Measurement of Electrode Reaction Kinetics *Anal. Chem.* **1965**, *37*, 1351-1355.

(4) Frisch, M. J. *Gaussian '09*, Revision B.01; Gaussian, Inc.: Wallingford, CT **2009**.

(5) Krishnan, R.; Binkley, J. S.; Seeger, R.; Pople, J. A. Self-Consistent Molecular-Orbital Methods .20. Basis Set for Correlated Wave-Functions *J Chem Phys* **1980**, *72*, 650-654.

(6) Mclean, A. D.; Chandler, G. S. Contracted Gaussian-Basis Sets for Molecular Calculations .1. 2nd Row Atoms, Z=11-18 *J Chem Phys* **1980**, *72*, 5639-5648.

(7) Zhao, Y.; Truhlar, D. G. The M06 suite of density functionals for main group thermochemistry, thermochemical kinetics, noncovalent interactions, excited states, and transition elements: two new functionals and systematic testing of four M06-class functionals and 12 other functionals *Theor Chem Acc* **2008**, *120*, 215-241.

(8) Marenich, A. V.; Cramer, C. J.; Truhlar, D. G. Universal Solvation Model Based on Solute Electron Density and on a Continuum Model of the Solvent Defined by the Bulk Dielectric Constant and Atomic Surface Tensions *J Phys Chem B* **2009**, *113*, 6378-6396.